JOURNAL OF Applied Polymer SCIENCE

Gas transport properties in (6FDA-RTIL)-(6FDA-MDA) block copolyimides

Caili Zhang,[1] Bing Cao,[1] Maria R. Coleman,[2] Pei Li[1]

[1]College of Materials Science and Engineering, Beijing University of Chemical Technology, Beijing 100029, China
[2]Department of Chemical and Environmental Engineering, the University of Toledo, Toledo, Ohio 43606
Correspondence to: P. Li (E-mail: lipei@mail.buct.edu.cn) and M. R. Coleman (E-mail: maria.coleman6@utoledo.edu)

ABSTRACT: This article reports synthesis and structure property studies of block copolyimides synthesized using diamino room temperature ionic liquids (RTIL) as diamine monomers. Specifically, polyimide oligomers of different lengths were synthesized using 2,2-bis (3,4-carboxylphenyl) hexafluoropropane dianhydride (6FDA) and diamino RTIL (1,3-di(3-aminopropyl) imidazolium bis[(trifluoromethyl) sulfonyl] imide). These oligomers were copolymerized with 6FDA and *m*-phenylenediamine (MDA) using *in situ* polymerization to form (6FDA-RTIL)-(6FDA-MDA) block copolyimides. The impact of the length and relative concentration of 6FDA-RTIL oligomer in the copolymer on the resulting thermal, physical, and gas transport properties was monitored. As the concentration of the 6FDA-RTIL segments increased, the backbone of the block copolyimides became more flexible resulting in a decrease in the glass transition temperature (T_g) and an increase in the density. The permeabilities of the RTIL containing copolyimides were consistently lower than those of the base polyimide, 6FDA-MDA, with some increase in selectivities. Interestingly, the permeabilities of films produced with the low molecular weight oligomers were very different than those produced with same composition of the high molecular weight oligomers. This may be indicative of very different morphologies within these copolyimides. © 2015 Wiley Periodicals, Inc. J. Appl. Polym. Sci. **2016**, *133*, 43077.

KEYWORDS: copolymers; glass transition; ionic liquids; membranes; polyimides

Received 24 August 2015; accepted 22 October 2015
DOI: 10.1002/app.43077

INTRODUCTION

RTILs have attracted considerable attention for use in gas separation membranes, especially for CO_2 separation because RTILs can be designed with high affinity to CO_2 simply through anion exchange reaction.[1–5] Many reports using RTILs in the applications of gas separation membranes focused on using them as the liquid phase of supported ionic liquid membranes (SILM) because of the low volatility and high thermal stability of RTIL. Some SILMs showed good CO_2/N_2 selectivities ranging from 20 to 50 with CO_2 permeabilities from 744 to 1200 Barrer.[6–14] While some SILMs have attractive potential transport properties, there are challenges of commercialization including weak mechanical stability, loss of RTIL at elevated temperatures and pressures and degradation of transport properties. Polymerized ionic liquid (PIL) has been extensively studied for membrane applications because it avoids issues of mechanical stability and loss of the membrane phase.[15–24] Some of these membranes exhibited separation performances for CO_2/N_2 gas pairs that surpassed the "1991 or 2008 Robeson upper bound."[25,26] Studies of PIL gas separation membranes are still limited but already demonstrate the potential for industrial applications.

In an earlier paper, our group reported a method of synthesizing two diamino RTILs monomers.[27] The RTILs were copolymerized with 6FDA and MDA to form random and block copolyimides whose structures were given in Figure 1(a,b).[27,28] The dicationic RTIL (diRTIL)-based random/block copolyimides exhibited significantly decreased permeabilities to CO_2 and a relatively small increased CO_2/CH_4 selectivity compared with the pure 6FDA-MDA. This was mainly due to the long alkyl groups in the diRTIL molecule which resulted in denser packing and higher chain flexibility.[27] Figure 1 shows that the monocationic RTIL (mRTIL) cation has fewer flexible alkyl groups compared with the diRTIL. As a result, the mRTIL-based copolyimides were expected to have more rigid backbones than those of the diRTIL-based copolyimides and exhibit a higher CO_2 permeability with similar CO_2/CH_4 or CO_2/N_2 selectivities compared with the diRTIL-based copolyimides. This work focuses on an investigation of physical and gas transport

Additional Supporting Information may be found in the online version of this article.

© 2015 Wiley Periodicals, Inc.

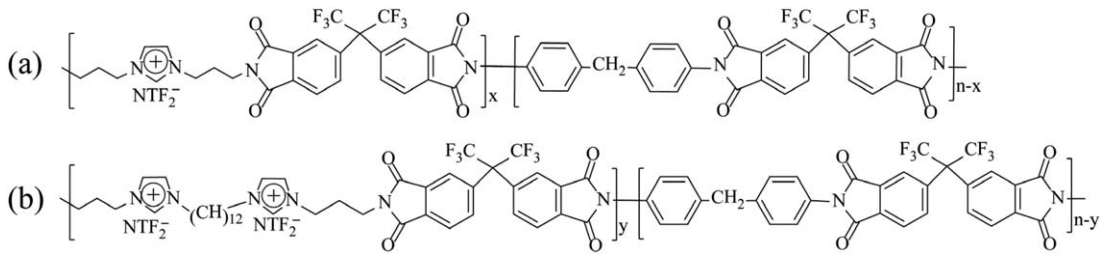

Figure 1. Structures of (a) (6FDA-mRTIL)-(6FDA-MDA) and (b) (6FDA-diRTIL)-(6FDA-MDA).

behavior of the mRTIL based copolyimides. In our previous study,[27] a 6FDA-mRTIL oligomer with a number molecular weight (M_n) of 2900 was synthesized and used to produce the (6FDA-MDA)-(6FDA-mRTIL) block copolyimides. In this work, a higher purity RTIL monomer was produced using methods in Ref. 26 which allowed synthesis of a higher molecular weight 6FDA-RTIL oligomer ($M_n = 6500$). The (6FDA-MDA)-(6FDA-mRTIL) long block copolyimides were synthesized using the high molecular weight 6FDA-mRTIL oligomer and short block copolyimides used the low molecular weight 6FDA-mRTIL. The polymer morphology and transport behavior of block copolyimides as a function of composition and block length are reported.

BACKGROUND

In block copolymers, penetrant transport properties are determined by the copolymer structure and the morphology of the microscale domain that can be formed by the component polymers. Specifically, for block copolymers, the morphology varies with changes in length of the segment block and chemical nature of the blocks.[29] Maxwell's model has been widely used to describe the permeability of block copolymers as a function of the permeabilities and concentration of the continuous/discontinuous phases.[30–33] The Maxwell–Wagner–Sillars equation is given in eq. (1).

$$P = P_c \cdot \frac{n \cdot P_d + (1-n) \cdot P_c + (1-n) \cdot (P_d - P_c) \cdot \varphi_c}{n \cdot P_d + (1-n) \cdot P_c - n \cdot (P_d - P_c) \cdot \varphi_d} \quad (1)$$

where P, P_c, and P_d are the permeabilities of the copolymer, continuous and discontinuous phase, respectively; n and φ_d the shape factor of the micro-scale discontinuous phase and the volume fraction of the discontinuous phase, respectively. This model can be simplified for specific morphologies shown in Figure 2 for block copolymers or analogously for mixed matrix materials.

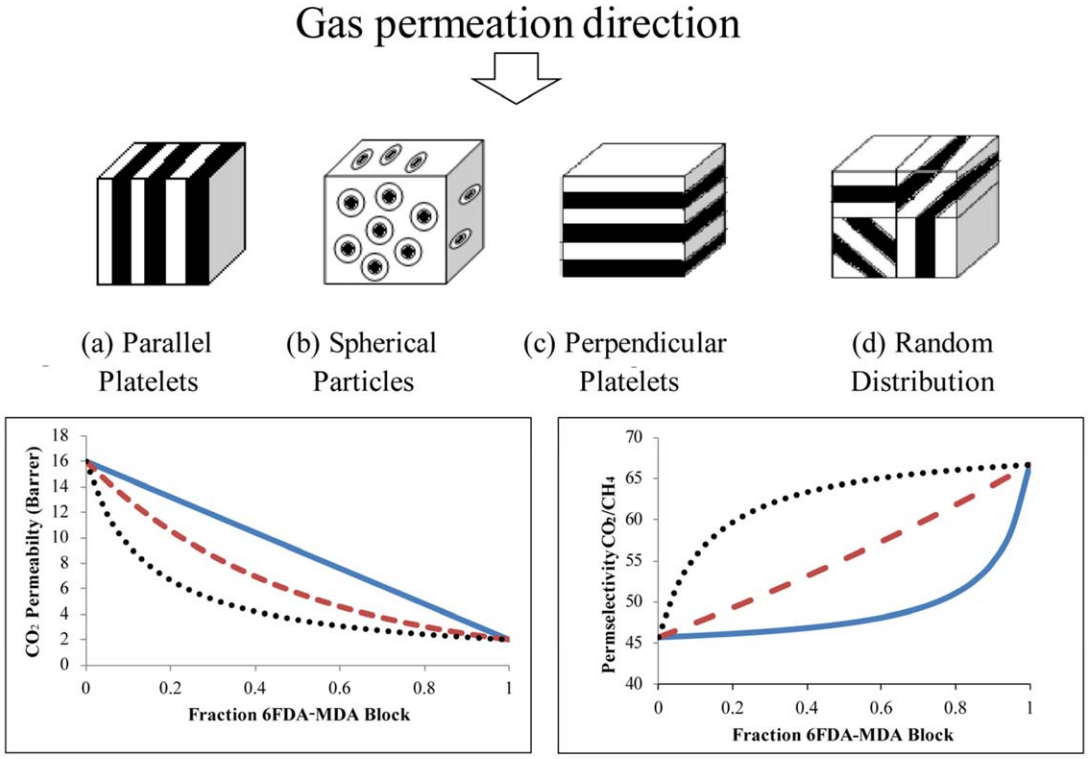

Figure 2. A schematic diagram of different heterogeneous morphologies and relationship between permeability and volume fraction of high permeable component in copolymer. Assuming the permeability of CO_2 in the two components are 2 and 16 Barrer and permeabilities of CH_4 are 0.03 and 0.35, respectively. The units of permeability are Barrer. The solid line represents case (a) parallel platelets, the dash line represents case (d) and the dotted line represents case (c) the perpendicular platelets. [Color figure can be viewed in the online issue, which is available at wileyonlinelibrary.com.]

The analogue of the relationship between the permeability and morphology in block copolymer has been studied in Bouma's work of mixed matrix polymers.[33] The equation can be simplified to eq. (2) with $n = 0$, when block copolymer forms platelet with the longest axis parallel to the cross membrane pressure. When the block copolymer forms platelets with the long axis perpendicular to the cross membrane pressure, the permeability is described by eq. (3) with $n = 1$. The gas permeability in random copolymer can be estimated using the semi-logarithmic additive rule in eq. (4).[30]

$$n=0: \quad P=P_c \cdot (1-\varphi_d)+P_d \cdot \varphi_d \tag{2}$$

$$n=1: \quad P=\frac{P_d \cdot P_c}{P_d \cdot (1-\varphi_d)+\varphi_d \cdot P_c} \tag{3}$$

$$\ln P=\varphi_1 \cdot \ln P_1+\varphi_2 \cdot \ln P_2 \tag{4}$$

where φ is the volume fraction and subscripts 1, 2 refer to the two component polymers.

Figure 2 demonstrates the effects of morphology and volume fraction on the permeability and permselectivity (the permeability selectivity of the low permeable component is assumed to be higher than that of the high permeable component). The parallel plate array exhibits the highest permeabilities and has a selectivity that is dominated by the values for the high permeability phase. For the case of platelets aligned perpendicular to the transport direction, the permeability and permeability selectivity are dominated by the properties of low permeability polymer over most concentrations. The random copolymers exhibit properties that are an average of values for individual components and are intermediate between the other cases shown in Figure 2. These models will be applied to elucidate the nature of morphology of the block copolymers reported herein.

EXPERIMENTAL SECTION

Materials

Pure gases, H_2, O_2, N_2, CH_4, and CO_2 purchased from Airgas, Inc. (Northwood, OH) with purities of 99.5% or greater were used as received. The 6FDA and MDA were purchased from Clariant LSM, (Gainesville, FL). Chemicals, di-tert-butyl dicarbonate, magnesium sulfurnate, 3-bromopropyl amine (hydrobromide), hydrobromic acid, ethyl acetate, tetrahydrofuran (THF), dimethylacetamide (DMAc), triethylamine (TEA), acetic anhydride (AA), methanol, 1,12-dibromododecane, isopropanol isopropanol, sodium hydroxide (NaOH) and sodium bicarbonate ($NaHCO_3$) were obtained from Sigma–Aldrich, (Milwaukee, WI). Lithium bis[tri(fluoromethane) sulfonyl]imide ($LiNTf_2$) was purchased from SynQuest Lab., (Alachua, FL). DMAc was refluxed under the protection of argon in the presence of CaH_2 for 3–4 h followed by distillation. TEA and AA were distilled to remove high boiling point impurities. The 6FDA and MDA were sublimed before polymerization.

Polymer Synthesis and Processing

Copolyimides with short and long blocks of 6FDA-mRTIL at concentrations up to 26 mol % were synthesized using a method described in a previous paper.[27] Specifically, the diamino mRTIL, 1,3-di(3-aminopropyl) imidazolium bis[(trifluoromethyl)sulfonyl]-imide, was synthesized and reacted with 6FDA to produce 6FDA-mRTIL oligomers with estimated 3.3 and 7.5 repeats units. The number of repeat units was estimated according to the M_n of the oligomers and the repeat unit. The 6FDA-mRTIL oligomer was further reacted with 6FDA and MDA using *in situ* polymerization to form copolyimides with a concentration of the 3.3 repeat unit 6FDA-mRTIL segments up to 26 mol %. These were referred to as short block copolyimides. A 6FDA-mRTIL oligomer with estimated 7.5 repeat units was synthesized and incorporated within block copolymers at concentrations up to 26 mol %. These were referred to as the long block copolyimides. The FTIR spectra and thermal stability of mRTIL monomer, 6FDA-mRTIL oliogmer, mRTIL based short and long block copolyimides and pure 6FDA-MDA were shown in Supporting Information.

Solution casting from dimethylchoride (MC) was used to produce films of the copolyimides for thermal-mechanical testing and gas transport studies. The polymers were dissolved in MC with a concentration of 5 wt %. After stirring for 12 h, the solution was filtered and placed in a glass dish kept in a glove bag. The solution was slowly evaporated for 2 days. The resulting films were placed into a vacuum oven at 80°C for 24 h and 200°C for 24 h to further evaporate the residual solvent.

Polymer Characterizations

The molecular weights were measured using a SCL-10Avp Shimadzu High-Performance Liquid Chromatography (GPC) purchased from Shimadzu Scientific Instrument (Columbia, MD) and calibrated using polystyrene standard samples. The M_n of the pure 6FDA-mRTIL oligomers were measured using THF as solvent and the M_n of the copolyimides were measured using MC as the solvent. The 6FDA-mRTIL oligomers were insoluble in MC and the copolyimides were sparingly soluble in THF; therefore, two solvent systems were used for GPC studies. Glass transition temperature (T_g) were measured using a Perkin Elmer Diamond DSC (Waltham, MA). The sample were heated at a rate of 30°C min^{-1} from 50 to 350°C and held at 350°C for 10 min to erase any thermal history. After cooling to 50°C at 30°C min^{-1}, the samples were heated at a slower heating rate of 20°C min^{-1}. The T_g values were obtained from the second heating curve. Multiple runs were obtained for each copolymer. The *d*-spacing was measured using a PANalytical X'Pert Pro MPD Powder X-ray diffractometer (WXAD) with a Cu Kα radiation wavelength of 1.54 Å. The *d*-spacing (d) was calculated using Bragg's equation, $n\lambda = 2d \sin\theta$, where $\lambda = 1.54$ Å, θ is the X-ray diffraction angle. The densities were determined using a density gradient column[34] with $Ca(NO_3)_2$ solutions. The fractional free volumes (FFV) of the block copolyimides were estimated using the method discussed in our previous paper.[28] The specific free volume (SFV), which was the product of the FFV and the polymer specific volume,[35] was utilized to correlate the gas transport properties of the copolyimides. Stern *et al.*[36] found that the SFV was a better parameter than the FFV for correlating the effects of side-chain substitutions in the diamine moiety on the gas permeability. In this work, the anion of the RTIL acted as a loosely bound side chain, which was analogous to the diamines used in Stern *et al.*'s work.[36] Therefore, both the FFV and SFV were utilized to analyze gas transport properties. Pure gas permeability was measured using a permeation cell with standard

Table I. T_g, *d*-spacing, Density, FFV, and SFV of the Block Copolyimides

Mol % of 6FDA-mRTIL	M_n	T_g (°C)	*d*-spacing (Å)	Density (g cm^{-3})	FFV	SFV (cm^3 g^{-1})
6FDA-MDA[a]	46,100 ± 1000	296 ± 2	5.60	1.394 ± 0.0001	0.1628	0.1168
Long block copolyimides						
6.5%	20,800 ± 300	278 ± 1	5.76	1.405 ± 0.0003	0.1595	0.1135
12.2%	35,500 ± 800	288 ± 2	5.81	1.408 ± 0.0002	0.1603	0.1138
25.8%	20,300 ± 400	275.8 ± 1.5	5.81	1.412 ± 0.0003	0.1637	0.1159
100%	6500 ± 200	-	-	1.473 ± 0.002	0.1517	0.1030
Short block copolyimides[a]						
6.5%	49,800 ± 1500	286.5 ± 0.5	5.47	1.402 ± 0.0005	0.1615	0.1152
14.8%	27,600 ± 900	281.7 ± 0.3	5.35	1.408 ± 0.0007	0.1606	0.1141
25.8%	21,700 ± 100	275.8 ± 1.2	5.32	1.417 ± 0.0005	0.1608	0.1135
100%	2900 ± 100	-	-	1.471 ± 0.002	0.1528	0.1038

[a] Data reported in a previous paper.[27]

methods described in detail elsewhere.[17] The downstream pressure was measured using a Barocel pressure sensor 600 AB trans 10TR purchased from Edwards (Troy, NY) with a full scale of 10 torr. Permeabilities for H_2, O_2, CO_2, N_2, and CH_4 were measured at 35°C and pressures up to 60 bar. The experimental procedures for measuring the gas permeability and solubility were described in our previous papers.[27,28] The gas diffusivities were determined from the permeability and solubility data using the correlation, $D = P/S$.

RESULTS AND DISCUSSION

Backbone Structures of the Block Copolyimides

Block copolyimides are synthesized with up to 26 mol % 6FDA-mRTIL and 6FDA-MDA using both short and long block 6FDA-mRTIL oligomers. The impact of block length and concentration on the microstructure, morphology and transport properties are characterized. The structure of the block copolyimides is shown in Figure 1(a). M_n as a function of compositions and 6FDA-mRTIL block lengths are given in Table I. M_n for the copolyimides tends to decrease with increasing 6FDA-mRTIL concentration with the exception of the copolyimide produced with 12 mol % 6FDA-mRTIL long block oligomer. This is consistent with earlier studies by our group. Note in all cases, the molecular weight of the copolymers is sufficiently high to allow formation of films for physical and gas transport property studies.

The backbone structure of the block copolyimides is affected by both the concentration and length of the 6FDA-mRTIL which is expected to affect the resulting properties. For example, a copolymer produced with low concentration of the long block 6FDA-mRTIL may result in the following two general populations of polyimide (i) pure 6FDA-MDA and (ii) copolymer which contains long 6FDA-mRTIL blocks and 6FDA-MDA blocks. As the concentration of 6FDA-mRTIL in the reaction mixture increases, the number of copolymer increases and the concentration of pure 6FDA-MDA decreases. The short block 6FDA-mRTIL is expected to produce copolyimides that are similar to random copolyimides particularly at higher concentrations of 6FDA-mRTIL.

The backbone structures of the copolymers are estimated using the M_n of the oligomer, copolyimides and the mol % of the 6FDA-mRTIL. The estimations are based on the following assumptions: (i) each molecule of the block copolyimide has the average M_n measured using GPC and (ii) every molecule tends to contain the lowest number of 6FDA-mRTIL oligomers. For example, each 6FDA-mRTIL block of the long block copolyimides has 7.5 repeat units. The M_n of the $(6FDA\text{-}mRTIL)_{7.5}$ and the 6FDA-MDA segments are 6500 and 610 respectively. For the block copolyimide containing one 6FDA-mRTIL block, the backbone structure of the 6.5 mol % long block copolyimide will be $(6FDA\text{-}MDA)_{11.8}$-$(6FDA\text{-}mRTIL)_{7.5}$-$(6FDA\text{-}MDA)_{11.8}$ because the average M_n of the polymer is 20,800.

Table II. Estimated Structures of the Repeat Units of the Block Copolyimides

Polymer	6FDA-mRTIL concentration	Backbone structures
Long block copolyimides	6.5 mol %	30 mol % [$A_{11.8}$-$B_{7.5}$-$A_{11.8}$] and 70 mol % [$A_{34.3}$]
	12.2 mol %	91 mol % [A_{24} -$B_{7.5}$-A_{24}] and 9 mol % [$A_{58.6}$]
	25.8 mol %	100 mol % $A_{11.5}$-$B_{7.5}$-$A_{11.5}$
Short block copolyimides	6.5 mol %	33 mol % [$A_{38.5}$-$B_{3.3}$-$A_{38.5}$] and 66 mol % [A_{24}-$B_{3.3}$-A_{24}-$B_{3.3}$-A_{24}]
	14.8 mol %	5 mol % [$A_{20.4}$-$B_{3.3}$-$A_{20.4}$] and 95 mol % [A_{12}-$B_{3.3}$-A_{12}-$B_{3.3}$-A_{12}]
	25.8 mol %	60 mol % [$A_{8.7}$-$B_{3.3}$-$A_{8.7}$-$B_{3.3}$-$A_{8.7}$] and 40 mol % [$A_{5.4}$-$B_{3.3}$-$A_{5.4}$-$B_{3.3}$-$A_{5.4}$-$B_{3.3}$-$A_{5.4}$]

A: (6FDA-MDA) B: (6FDA-mRTIL).

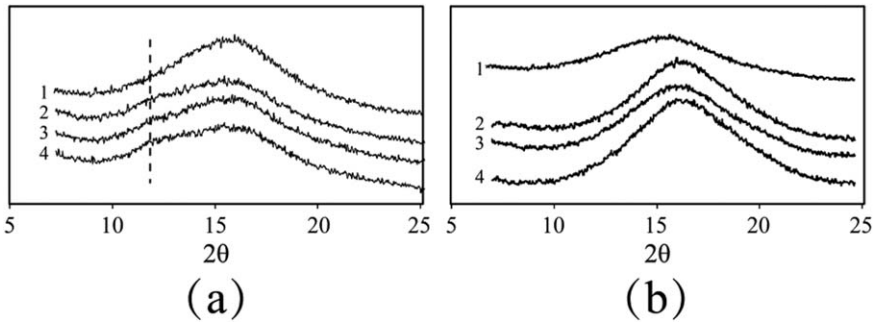

Figure 3. (a) Wide angle X-ray diffraction patterns of (1) 6FDA-MDA, (2) 6.5 mol %, (3) 12.2 mol %, and (4) 25.8 mol % long block copolyimides. (b) Wide angle X-ray diffraction patterns of (1) 6FDA-MDA, (2) 6.5 mol %, (3) 14.8 mol % and (4) 25.8 mol % short block copolyimides.

However, the 6FDA-mRTIL molar concentration in this mono-block copolyimide will be 24 mol % based on the backbone structure which is much higher than 6.5 mol % for this copolyimide. Therefore, a 6.5 mol % long block copolyimide reaction mixture shall include a mixture of the mono-block copolyimide described above and pure 6FDA-MDA that has an average M_n of 20,800 and a structure of (6FDA-MDA) 34.3. The molar concentrations of the mono-block copolyimides and the pure 6FDA-MDA have to be 30 mol % and 70 mol % to fit the overall 6FDA-mRTIL concentration of 6.5 mol % and the M_n of 20 800. Using this method, the backbone structures and their molar concentrations of both the long block and the short block copolyimides are estimated and listed in Table II. The purpose of this analysis is to demonstrate that the natures of copolyimide structures are very different for the long and short block polymers which are expected to impact the polymer morphology, physical and transport properties. For instance, Fan *et al.*[37] synthesized a series of sulfonated poly(arylene ether sulfone)s block copolymers. They reported that the morphologies of the block copolymers turned from homogeneous into heterogeous as the block lengths increased from 5 K to 10 K and 15 K. Chung *et al.* studied the miscible properties of a series of PIM-1/Ultem and PIM-1/Matrimid polymer blends and observed that the polymer blends were homogeneous as the concentration of minority component was <5 wt %.[38,39] When the concentration increased, the polymer blends became heterogenous. In this study, we also observe different phase behaviors between the short and long block copolyimides that will be discussed in detail later.

Physical Properties of the Short and Long Block Copolyimides

Many block copolyimides can exhibit more than one T_g and each T_g is assigned to the component polymers because of micro phase separation occurs.[30,40] In this study, all of the block copolyimides exhibit a single T_g. This may be due to the small size of the 6FDA-mRTIL blocks which makes their T_g difficult to detect. Note that, the T_g of the 6FDA-mRTIL oligomers are also undetectable using DSC.

As shown in Figure 1, the 6FDA dianhydride contains fluorinated groups [-C(CF_3)$_2$-] which are bulky and hinder the rotational mobility of the polymer backbone. In 6FDA-MDA segment, the bonds linking the nitrogen and benzene ring and the alkyl group connecting the two benzene groups in MDA are the most flexible positions that allow the polymer backbone to rotate. The mRTIL possesses six alkyl groups, hence the 6FDA-mRTIL block has multiple positions that favor rotational mobility of the polymer backbone. As shown in Table I, a general trend is observed that the T_g gradually decreases with an increase in the 6FDA-mRTIL mol % for both sets of copolyimides. This is consistent with the presence of flexible aliphatic groups in the 6FDA-mRTIL segments. The 6.5 mol % long block copolyimide exhibits lower T_g compared to those of the 6.5 mol % short block copolyimide. The difference in T_g may be due to the much lower M_n of the long block copolyimide at similar concentration. The impact of the M_n on T_g were reported by Fox and Flory[41] who claimed that polymers having similar chemical structures had a lower T_g at low molecular weight. This is attributed to the excess free volumes around the polymer chain ends. Therefore, the low T_g of the 6.5 mol % long block copolyimide may stem from its low M_n. And the low T_g of the long block copolyimide may cause denser packing than that of the short block copolyimide at 6.5 mol %.

Polymer Morphology and *d*-spacing

The WAXD patterns of the pure 6FDA-MDA and the long block copolyimides are given in Figure 3(a) and those of the short block copolyimides are given in Figure 3(b). In amorphous polymers, long range order does not exist, and only short range order, which is formed by the average distance between polymer chains, is present.[42] As shown in Table I, the *d*-spacing of the long block copolyimides increases with increasing 6FDA-mRTIL mol %. The WAXD spectra of the long block copolyimides

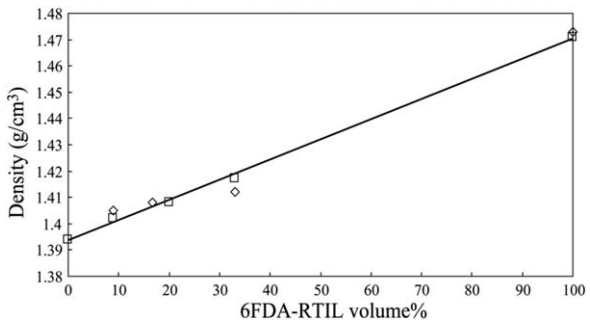

Figure 4. Relationship between the density and the 6FDA-RTIL volume fraction (□) the short block copolyimides (◇) the long block copolyimides.

Table III. Comparison of Permeabilities, Solubilities, Diffusivities, and their Selectivities for O_2/N_2 Gas Pair in Various Copolyimides at 35°C and 10 atm (O_2 at 2 atm)

Polymer	PO_2 (Barrers)	$\frac{P_{O_2}}{P_{N_2}}$	SO_2 [cm^3(stp)/cm^3 (polymer) atm]	$\frac{S_{O_2}}{S_{N_2}}$	DO_2 $\times 10^{10}$ cm^2 s^{-1})	$\frac{D_{O_2}}{D_{N_2}}$
6FDA-MDA	3.63	5.7	0.75	1.70	4.84	3.3
6.5 mol %-L	2.29	5.9	0.78	1.50	2.93	3.9
12.2 mol %-L	1.98	6.2	0.83	1.47	2.38	4.2
25.8 mol %-L	1.89	6.3	0.84	1.42	2.25	4.4
6.5 mol %-S	3.51	5.7	0.77	1.57	4.56	3.6
14.8 mol %-S	2.82	6.0	0.80	1.45	3.52	4.1
25.8 mol %-S	2.48	6.0	0.83	1.38	2.98	4.4

L-long block copolyimides; S-short block copolyimides.

exhibits a broad peak at 15.3° (*d*-spacing of 5.80 Å) and a shoulder peak at 11.5° (*d*-spacing of 7.7 Å).

For the short block copolyimides, the 2θ gradually increases to 16.5° at 25.8 mol % for a *d*-spacing of 5.32 Å and all the peaks are sharp and symmetric. The short block copolyimides appear to be homogenous without indication of separate packing environments. The *d*-spacing of the short block copolyimides decreases with increasing the 6FDA-mRTIL concentrations. This is consistent with the incorporation of the aliphatic groups of the mRTIL that allows for rearrangement of polymer chain during cooling and denser packing of the copolyimides. The x-ray diffraction and *d*-spacing results indicate that there may be substantive differences in the packing morphology of the long and short block copolyimides.

Density and FFV/SFV

The density of miscible polymer blends or homogeneous copolymers is often found to linearly correlate with the volume fraction of one component.[30] As shown in Figure 4, the densities of the short block copolyimides correlate linearly with the 6FDA-mRTIL volume fraction. However, the densities of the long block copolyimides deviate from the linear relations especially at 25.8 mol %. Similar to the WAXD analysis, these results may also indicate that the morphology of the short block copolyimides is homogeneous and that of the long block copolyimides is heterogeneous.

According to Table I, the FFVs/SFVs of the long/short 6FDA-mRTIL oligomers are much smaller than those of the pure 6FDA-MDA. This is consistent with the more flexible backbones and higher densities of the 6FDA-mRTIL oligomers. The FFVs of the short block copolyimides are smaller than the pure 6FDA-MDA at concentrations up to 25.8 mol %. The SFVs of the short block copolyimides gradually decrease with 6FDA-mRTIL mol %. This is consistent with a homogenous polymer with an increased chain flexibility and denser packed structure. The FFVs/SFVs of the long block copolyimides increase with an increase in the 6FDA-mRTIL mol % although the FFV/SFV of the oligomer is much lower than the pure 6FDA-MDA. At 25.8 mol %, the FFV of the long block copolyimide is even greater than the pure 6FDA-MDA. This may be due to the formation of regions of high free volume because of the presence large rigid 6FDA-MDA blocks that cannot readily pack and the flexible 6FDA-mRTIL domains that allow for regions of dense packing.

Gas Transport Properties

Permeabilities. The pure gas permeabilities, solubilities, diffusivities, and their corresponding selectivities of the short/long block copolyimides and pure 6FDA-MDA are given in Tables (III–VI). The permeabilities gradually decrease and the permeability selectivities increase with an increase in the 6FDA-mRTIL mol % of the block copolyimides. The short block copolymers follow a trade-off relationship between the permeability and selectivity. This may be attributed to the

Table IV. Comparison of Permeabilities, Solubilities, Diffusivities, and their Selectivities for CO_2/CH_4 Gas Pair in Various Copolyimides at 35°C and 10 atm

Polymer	PCO_2 (Barrers)	$\frac{P_{CO_2}}{D_{CH_4}}$	SCO_2 [cm^3(stp)/cm^3 (polymer) atm]	$\frac{S_{CO_2}}{S_{CH_4}}$	DCO_2 ($\times 10^8$ cm^2 s^{-1})	$\frac{D_{CO_2}}{D_{CH_4}}$
6FDA-MDA	15.8	44.9	4.28	3.67	3.70	12.2
6.5 mol %-L	9.08	53.4	3.92	2.95	2.31	18.1
12.2 mol %-L	8.18	68.2	3.73	2.52	2.19	27.1
25.8 mol %-L	7.22	72.2	3.48	2.19	2.08	33.0
6.5 mol %-S	14.4	46.6	4.00	3.03	3.61	15.4
14.8 mol %-S	11.7	55.6	3.64	2.46	3.21	22.6
25.8 mol %-S	9.18	61.5	3.68	2.34	2.49	26.3

L-long block copolyimides; S-short block copolyimides.

Table V. Comparison of Permeabilities, Solubilities, Diffusivities, and their Selectivities for N_2/CH_4 Gas Pair in Various Copolyimides at 35°C and 10 atm

Polymer	PN_2 (Barrers)	$\frac{P_{N_2}}{D_{CH_4}}$	SN_2 [cm^3(stp)/cm^3 (polymer) atm]	$\frac{S_{N_2}}{S_{CH_4}}$	DN_2 ($\times 10^8$ cm^2 s^{-1})	$\frac{D_{N_2}}{D_{CH_4}}$
6FDA-MDA	0.64	1.83	0.44	0.38	1.45	4.84
6.5 mol %-L	0.39	2.29	0.52	0.39	0.74	5.82
12.2 mol %-L	0.32	2.67	0.56	0.38	0.57	7.02
25.8 mol %-L	0.30	3.0	0.59	0.37	0.51	8.17
6.5 mol %-S	0.62	2.0	0.49	0.37	1.27	5.47
14.8 mol %-S	0.47	2.24	0.55	0.37	0.85	6.07
25.8 mol %-S	0.41	2.73	0.60	0.38	0.68	7.56

L-long block copolyimides; S-short block copolyimides.

incorporation of the high flexible 6FDA-mRTIL segments that decreases the SFVs of the short copolyimide. This is consistent with other physical properties discussed above and impact of composition on random copolymers.

The long block copolyimides have much lower permeabilities and higher permeability selectivities than the short block copolyimides. However, no clear relation between SFV and permeability is found for the long block copolyimides. The permeabilities gradually decrease but the SFVs of the long block copolyimides continuously increase with an increase in the 6FDA-mRTIL concentration. Therefore, the overall free volume does not reflect the change in gas transport properties of the long block copolyimides. This is a typical phenomenon for block copolymers where the polymer segments form different domains.[31–33] In these situations, the gas transport behaviors are dependent on the morphologies and compositions of the block copolymers. The permeability results may indicate that the long block copolyimides have a very different free volume distribution in which the following two primary domains can be envisioned: dense packed 6FDA-mRTIL rich domains and loosely packed 6FDA-MDA rich domains. Because the permeabilities are much lower than the short block copolyimides, the gas permeabilities of the long block copolyimides are mainly controlled by the densily packed 6FDA-mRTIL domains.

As shown in Figure 5, the permeabilities of the short block copolyimides fit the linear curves which are estimated using the semilogarithmic rule where the permeabilities of the pure 6FDA-mRTIL are estimated by extrapolation from the permeabilities of the short block copolyimides. It indicates that the morphology is random or homogeneous. The 6FDA-MDA block and the 6FDA-mRTIL block are well mixed without the formation of domains and phase separations. The permeability coefficients of the long block copolyimides fit the convex curves which are estimated using eq. (3), especially at 6.5 and 14.8 mol %. These results may indicate that the 6FDA-mRTIL block and 6FDA-MDA block of the long block copolyimides form different domains. The 6FDA-mRTIL domains are more densely packed and possess low permeability. The 6FDA-MDA domains are loosely packed and exhibit high permeability. Because at similar oligomer loadings, the long block copolyimides exhibit much lower permeabilities than those of the short block copolyimides, the permeabilities of the long block copolyimides are mainly controlled by the low permeable 6FDA-mRTIL domains. At 25.8 mol %, the permeabilities of long block copolyimide are close to the linear fitting curves. It may indicate that its morphology is different to those of the 6.5 and 14.8 mol % long block copolyimides. Note that, the 25.8 mol % long block copolyimide is a pure block copolyimide similar to the short block copolyimides but different to the 6.5 and 14.8 mol % long block copolyimides which consist of two populations (i.e., block copolyimides and pure 6FDA-MDA shown in Table II). Therefore, the morphology of the 25.8 mol % long block copolyimides may be similar to the short block copolyimides.

Table VI. Comparison of Permeabilities, their Selectivities for H_2/CH_4 Gas Pair and the Solubilities/Diffusivities of the CH_4 in Various Copolyimides at 35°C and 10 atm

Polymer	PH_2 (Barrers)	$\frac{P_{H_2}}{P_{CH_4}}$	SCH_4 [cm^3(stp)/cm^3 (polymer) atm]	DCH_4 ($\times 10^8$ cm^2 s^{-1})
6FDA-MDA	40.2	114.1	1.16	0.30
6.5 mol %-L	23.6	138.9	1.33	0.13
12.2 mol %-L	18.8	156.3	1.47	0.08
25.8 mol %-L	17.3	173.2	1.59	0.06
6.5 mol %-S	36.6	118.0	1.32	0.23
14.8 mol %-S	31.2	148.6	1.48	0.14
25.8 mol %-S	27.7	184.8	1.57	0.09

L-long block copolyimides; S-short block copolyimides.

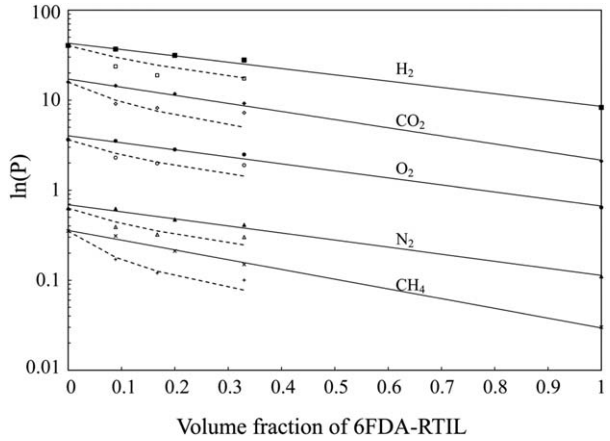

Figure 5. The relationships between the logarithmic permeability and oligomer volume fraction. The solid points represent the short block copolyimides and the empty points attributed to the long block copolyimides. Linear lines were the fitting curves using semilogarithmic rule [eq. (4)] and the convex curves are the fitting result using Maxwell model [eq. (1)].

Solubilities. The solubilities of all gases follow similar trends and values for both the short and long block copolyimides with increasing 6FDA-mRTIL oligomer loading. There is a general trend for O_2, N_2 and CH_4 to increase with increasing loading and for CO_2 to decrease with increasing 6FDA-mRTIL loading. For example, the solubilities of O_2, N_2 and CH_4 are 12, 35, and 37% higher, respectively, for the 25.8% 6FDA-mRTIL oligmer than the pure 6FDA-MDA Interestingly, the solubilities of CO_2 show a very different trend with a decrease of 19% relative to pure 6FDA-MDA. The solubility selectivities of O_2/N_2 and CO_2/CH_4 gas pairs decrease to 83 and 60%, while that of N_2/CH_4 gas pair does not change. Therefore, CO_2 is the only gas that has lower solubility and the solubility selectivities of the block copolyimides are smaller than the pure 6FDA-MDA. To investigate the gas sorption behavior, the dual-mode sorption model is applied to the sorption isotherms to probe the nature of sorption environment in the copolymers.[39]

The sorption isotherms to CO_2, CH_4, and N_2 of the short and long block copolyimides are plotted in Figure 6(a,b) where the solid lines are the curve fitting results using the Dual-Mode sorption model as given in eq. (5).

$$C = k_D \cdot p + \frac{C'_H \cdot b \cdot p}{1 + b \cdot p} \tag{5}$$

where k_D, C'_H, and b are the Henry law constant, Langmuir capacity parameter, and Langmuir mode affinity constant. Gas absorbed in the Henry mode is similar to the gas dissolution in a liquid where solubility increases linearly with pressure, while gas adsorbed in the Langmuir mode has a capacity limit because it behaves like a hole filling process. The estimated dual-mode parameters are given in Table VII. All sorption isotherms concave to the x axis which is a typical behavior for glassy polymers that obey the dual-mode sorption mechanism.

According to Table VII, The Langmuir sorption capacity (C'_H) of CO_2, CH_4, and N_2 are all higher than that of the pure 6FDA-MDA except for those of CO_2 of the long block copolyimides. C'_H of all gases for the short block copolyimides gradually increase with the 6FDA-mRTIL mol % which may indicate the excess free volumes gradually increase. Because the FFVs of the short block copolyimides gradually decrease and the total free volume of a glass polymer is the summary of the normal and excess free volumes, the normal free volume shall decrease with

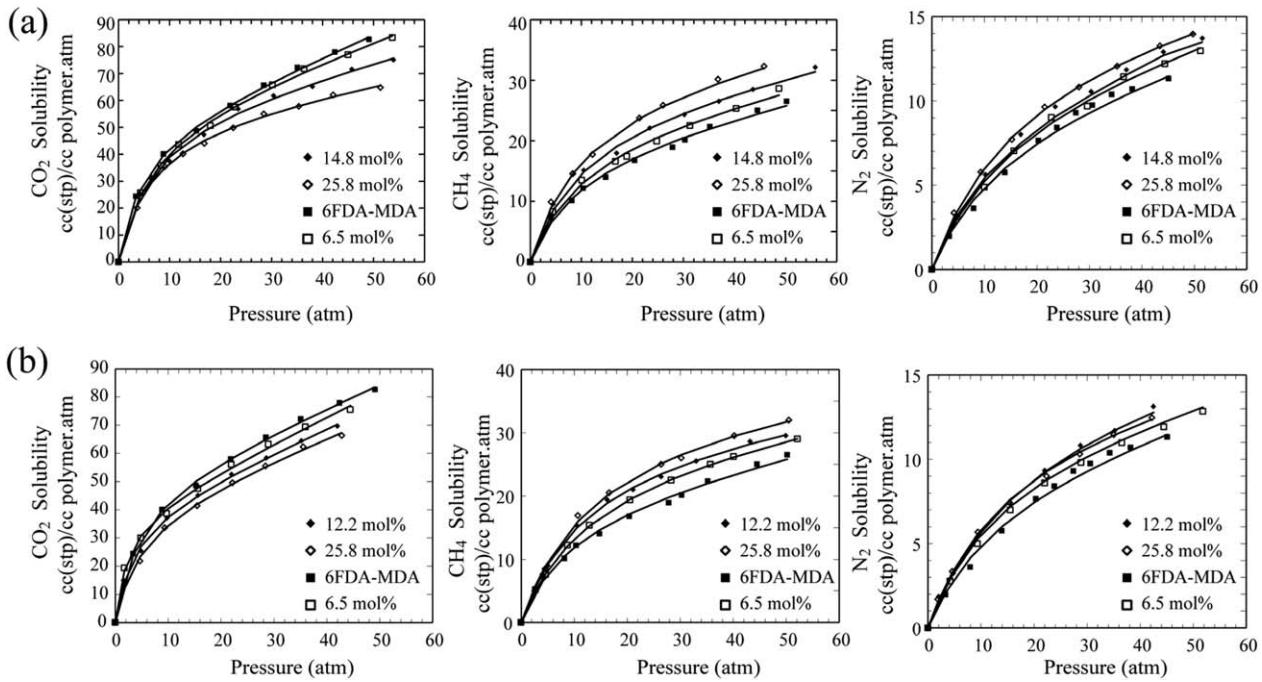

Figure 6. (a) CO_2, CH_4 and N_2 solubility of the pure 6FDA-MDA and the short block copolyimides; (b) CO_2, CH_4 and N_2 solubility of the pure 6FDA-MDA and the long block copolyimides. The solid lines represent the fitting curve using the dual mode model.

the increase in 6FDA-mRTIL mol %. This is also proved by the smaller *d*-spacing of the short block copolyimides. The decrease in k_D of the short block copolyimides with an increase in the 6FDA-mRTIL concentration is consistent with this decrease in *d*-spacing and greater chain packing. Note that, the larger decrease in the k_D of CO_2 may be also due to the low CO_2-copolyimide interaction. In Table VII, with the addition of the 6FDA-mRTIL segments, the hole affinity "*b*" of N_2 and CH_4 do not change much, while that of the CO_2 gradually decreases for the short block copolyimide. It indicates that the CO_2-copolyimide interactions decrease with the incorporation of 6FDA-mRTIL segments. For the long block copolyimides, C'_H to N_2 and CH_4 increase with increasing the 6FDA-mRTIL mol % that is similar to the short block copolyimide. However, C'_H to CO_2 of the long block copolyimides are smaller than that of 6FDA-MDA. The reason is unclear at this moment.

Diffusivities. As the concentrations of the 6FDA-mRTIL for both classes of copolyimides increase, there are general decreases in diffusivities with a corresponding increase in diffusivity selectivities. Specifically, the diffusivities of CO_2, O_2, N_2, and CH_4 decrease by 56, 46, 35, and 20%, respectively for the long block copolyimide with 25.8% 6FDA-mRTIL relative to the pure 6FDA-MDA. The diffusivity selectivities of O_2/N_2, CO_2/CH_4, and N_2/CH_4 gas pairs increase about 33, 179, and 60%, respectively. For the short block copolyimides, as the 6FDA-mRTIL increase to 25.8 mol %, the diffusivities of CO_2, O_2, N_2 and CH_4 gradually decrease to 67, 61, 47, and 30% relative to the pure 6FDA-MDA, respectively. The diffusivity selectivities of O_2/N_2, CO_2/CH_4 and N_2/CH_4 gas pairs increase 31, 116, and 56%, respectively. The diffusivities of the big molecules (CH_4, N_2) exhibit larger decreases than those of the small molecules (O_2, CO_2). In addition, diffusivities of the long block copolyimides are lower than those of the short block copolyimides at the similar 6FDA-mRTIL mol %. The diffusivity selectivities gradually increase with the increase in 6FDA-mRTIL mol %. And the bigger size difference between the gas pair results in the more increase in the diffusivity selectivity. The block copolyimides become more size selective compared with the pure 6FDA-MDA.

Table VII. Dual-mode Model Parameters of the Block Copolyimides and Pure 6FDA-MDA at 35°C

Polymer	k_D (cm^3(STP)/cm^3 (polymer) atm)	C'_H (cm^3(STP)/cm^3 (polymer))	*b* (1/atm)
N_2			
6FDA-MDA	0.090	9.85	0.067
6.5 mol %-S	0.082	11.89	0.059
14.8 mol %-S	0.073	12.94	0.064
25.8 mol %-S	0.055	15.35	0.055
6.5 mol %-L	0.079	11.48	0.070
12.2 mol %-L	0.060	14.86	0.052
25.8 mol %-L	0.055	13.94	0.061
CH_4			
6FDA-MDA	0.181	20.08	0.099
6.5 mol %-S	0.172	23.42	0.091
14.8 mol %-S	0.165	26.37	0.095
25.8 mol %-S	0.159	30.58	0.092
6.5 mol %-L	0.140	27.32	0.08
12.2 mol %-L	0.107	30.43	0.08
25.8 mol %-L	0.09	35.22	0.07
CO_2			
6FDA-MDA	0.787	48.68	0.228
6.5 mol %-S	0.657	54.40	0.158
14.8 mol %-S	0.433	54.84	0.141
25.8 mol %-S	0.321	55.31	0.151
6.5 mol %-L	0.677	48.49	0.259
12.2 mol %-L	0.804	39.47	0.289
25.8 mol %-L	0.723	40.50	0.205

L refers to the long block copolyimides and S refers to the short block copolyimides.

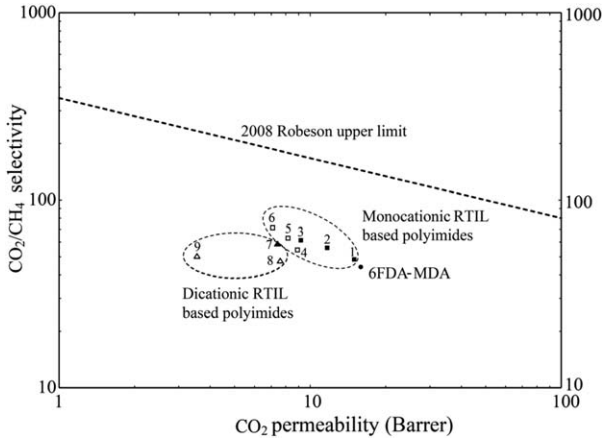

Figure 7. Separation performance to CO_2/CH_4 gas pair for RTIL based copolyimides using Robeson trade-off relations. 1, 2, 3 are 6.5, 14.8, and 25.8 mol % short block copolyimides;4, 5, and 6 are 6.5, 12.2, and 25.8 mol % long block copolyimides; 7, 8, and 9 are diRTIL based copolyimides reported from literature.[25,26]

Comparison of the Separation Performance between mRTIL and diRTIL-based Copolyimides

The separation performance of all mRTIL and diRTIL-based copolyimides for the CO_2/CH_4 gas pair is presented in Figure 7 using the trade-off curve developed by Robeson *et al.* The data points are all under "the 2008 Robeson upper bound."[25] However, the performance of all mRTIL based block copolyimides is closer to the upper bond than the diRTIL-based copolyimides (points 7, 8, and 9) that match our expectation: the mRTIL based polyimides have less flexible backbones then those of the diRTIL-based polyimides; therefore, the separation performance of the former is better than the latter.

CONCLUSIONS

Series of mRTIL based (6FDA-MDA)-(6FDA-mRTIL) short/long block copolyimides were successfully synthesized and characterized. The impact of 6FDA-mRTIL oligomer length and

concentration on the block copolyimides was investigated and results were discussed in terms of changes in polymer structure and morphology.

The polymer morphologies of the long block copolyimides are very different from the short block copolyimides at similar concentrations. Interestingly, the 25.8 mol % long block copolyimide exhibits higher FFV and SFV than those of the pure 6FDA-MDA. This is consistent with formation of very different morphologies for the long block copolyimides with regions of dense packing due to the flexible 6FDA-mRTIL blocks and regions of open packing due to the 6FDA-MDA blocks.

These differences in chain packing in the short and long block copolyimides result in very different gas transport properties at similar oligomer concentrations. Specifically, the permeabilities of the long block copolyimides fit the prediction of the Maxwell model, which indicates that the lower permeability dense packed 6FDA-mRTIL domains mainly determine the transport properties. While, permeabilities of the short block copolyimides fit the predication of the semilogarithmic rule, which indicates that the polymer morphologies are homogeneous and behave as a random copolyimide.

The gas permeability gradually decreases as the 6FDA-mRTIL mol % of the block copolyimides increases and associates with the increase of the permeability selectivity of O_2/N_2, N_2/CH_4 and CO_2/CH_4 gas pairs. The permeabilities of the long block copolyimides are lower than those of the short block copolyimides. However, the permeability selectivities in the long block copolyimides are higher. The relations of permeability and selectivity are in the agreement with the Robeson trade off relationship. One significant improvement on the selectivity of CO_2/CH_4 is observed. The FFV and SFV didn't correlate the permeabilities of the long block copolyimides which may be due to the formation of regions of localized phase separations. For the short block copolyimides, the permeability gradually decreases with the decrease in the SFVs caused by the increase in the 6FDA-mRTIL mol %. It indicates that a decrease in the normal free volume which favors the transport of gas molecules.

Gas solubilities are similar for the short and long block copolyimides at the similar 6FDA-mRTIL mol %. The block copolyimides show higher solubility to O_2, N_2, and CH_4 but lower solubility to CO_2 than the pure 6FDA-MDA. The regression parameters of the Dual-Mode sorption model indicate that C'_H of all gases of the short block copolyimides are greater than that of the pure 6FDA-MDA. This means that the excess free volumes of the short block copolyimides are greater than that of the pure 6FDA-MDA. The decrease in CO_2 solubility may be due to the decrease in the CO_2-copolyimide interaction and the decrease in the normal free volume. The diffusivities of all gases decrease in the block copolyimides. The diffusivities of the long block copolyimides are smaller than those of the short block copolyimides. And the diffusivity selectivities of the long block copolyimides are higher.

ACKNOWLEDGMENTS

The authors thank the National Natural Science Foundation of China (51403012) to support this research.

REFERENCES

1. Blanchard, L. A.; Hancu, D.; Beckman, E. J.; Brennecke, J. F. *Nature* **1999**, *399*, 28.
2. Hudiono, Y. C.; Carlisle, T. K.; LaFrate, A. L.; Gin, D. L.; Noble, R. D. *J. Membr. Sci.* **2011**, *370*, 141.
3. Miller, A.; Carlisle, T.; LaFrate, A.; Voss, B.; Bara, J.; Hudiono, Y.; Wiesenauer, B.; Gin, D.; Noble, R. *Sep. Sci. Technol.* **2012**, *47*, 169.
4. Yoo, S.; Won, J.; Kang, S. W.; Kang, Y. S.; Nagase, S. *J. Membr. Sci.* **2010**, *363*, 72.
5. Hao, L.; Li, P.; Yang, T.; Chung, T. S. *J. Membr. Sci.* **2013**, *436*, 221.
6. Santos, E.; Albo, J.; Irabien, A. *J. Membr. Sci.* **2014**, *452*, 277.
7. Zhao, W.; He, G.; Nie, F.; Zhang, L.; Feng, H.; Liu, H. *J. Membr. Sci.* **2012**, *411*, 73.
8. Moganty, S. S.; Chinthamanipeta, P. S.; Vendra, V. K.; Krishnan, S.; Baltus, R. E. *Chem. Eng. J.* **2014**, *250*, 377.
9. Chae, I. S.; Lee, J. H.; Hong, J.; Kang, Y. S.; Kang, S. W. *Chem. Eng. J.* **2014**, *251*, 343.
10. Lan, W.; Li, S.; Xu, J.; Luo, G. *Ind. Eng. Chem. Res.* **2013**, *52*, 6770.
11. Jindaratsamee, P.; Ito, A.; Komuro, S.; Shimoyama, Y. *J. Membr. Sci.* **2012**, *423*, 27.
12. Scovazzo, P.; Havard, D.; McShea, M.; Mixon, S.; Morgan, D. *J. Membr. Sci.* **2009**, *327*, 41.
13. Bara, J. E.; Gabriel, C. J.; Carlisle, T. K.; Camper, D. E.; Finotello, A.; Gin, D. L.; Noble, R. D. *Chem. Eng. J.* **2009**, *147*, 43.
14. Scovazzo, P.; Kieft, J.; Finan, D. A.; Koval, C.; DuBois, D.; Noble, R. *J. Membr. Sci.* **2004**, *238*, 57.
15. Yuan, J.; Mecerreyes, D.; Antonietti, M. *Prog. Polym. Sci.* **2013**, *38*, 1009.
16. Tomé, L. C.; Mecerreyes, D.; Freire, C. S.; Rebelo, L. P. N.; Marrucho, I. M. *J. Membr. Sci.* **2013**, *428*, 260.
17. Crick, C. R.; Parkin, I. P. *Thin Solid Films* **2010**, *518*, 4328.
18. Chen, H. Z.; Li, P.; Chung, T. S. *Int. J. Hydrogen Energy* **2012**, *37*, 11796.
19. Li, P.; Pramoda, K.; Chung, T. S. *Ind. Eng. Chem. Res.* **2011**, *50*, 9344.
20. Carlisle, T. K.; Bara, J. E.; Lafrate, A. L.; Gin, D. L.; Noble, R. D. *J. Membr. Sci.* **2010**, *359*, 37.
21. Bara, J. E.; Gabriel, C. J.; Hatakeyama, E. S.; Carlisle, T. K.; Lessmann, S.; Noble, R. D.; Gin, D. L. *J. Membr. Sci.* **2008**, *321*, 3.
22. Bara, J. E.; Lessmann, S.; Gabriel, C. J.; Hatakeyama, E. S.; Noble, R. D.; Gin, D. L. *Ind. Eng. Chem. Res.* **2007**, *46*, 5397.
23. Hu, X.; Tang, J.; Blasig, A.; Shen, Y.; Radosz, M. *J. Membr. Sci.* **2006**, *281*, 130.
24. Mecerreyes, D. *Prog. Polym. Sci.* **2011**, *36*, 1629.
25. Robeson, L. M. *J. Membr. Sci.* **2008**, *320*, 390.
26. Robeson, L. M. *J. Membr. Sci.* **1991**, *62*, 165.

27. Li, P.; Zhao, Q.; Anderson, J. L.; Varanasi, S.; Coleman, M. R. *J. Polym. Sci. A* **2010**, *48*, 4036.
28. Li, P.; Coleman, M. R. *Eur. Polym. J.* **2013**, *49*, 482.
29. Niwa, M.; Nagaoka, S.; Kawakami, H. *J. Appl. Polym. Sci.* **2006**, *100*, 2436.
30. Paul, D. *J. Membr. Sci.* **1984**, *18*, 75.
31. Barrie, J.; Ismail, J. *J. Membr. Sci.* **1983**, *13*, 197.
32. Barnabeo, A.; Creasy, W.; Robeson, L. *J. Polym. Sci. Polym. Chem.* **1975**, *13*, 1979.
33. Bouma, R.; Checchetti, A.; Chidichimo, G.; Drioli, E. *J. Membr. Sci.* **1997**, *128*, 141.
34. ASTM D 1928-90. Standard Practice for Preparation of Compression Molded Polyethylene Test Sheets and Test Specimens, Annual Book of ASTM Standards 08.02; **1992**.
35. Lee, W. *Polym. Eng. Sci.* **1980**, *20*, 65.
36. Stern, S.; Liu, Y.; Feld, W. *J. Polym. Sci. B: Polym. Phys.* **1993**, *31*, 939.
37. Fan, Y.; Cornelius, C. J.; Lee, H. S.; McGrath, J. E.; Zhang, M.; Moore, R.; Staiger, C. L. *J. Membr. Sci.* **2013**, *430*, 106.
38. Yong, W.; Li, F.; Xiao, Y.; Li, P.; Pramoda, K.; Tong, Y.; Chung, T. *J. Membr. Sci.* **2012**, *407*, 47.
39. Hao, L.; Li, P.; Chung, T. S. *J. Membr. Sci.* **2014**, *453*, 614.
40. Bondar, V.; Freeman, B.; Pinnau, I. *J. Polym. Sci. B Polym. Phys.* **2000**, *38*, 2051.
41. Fox, T. G., Jr.; Flory, P. J. *J. Appl. Phys.* **1950**, *21*, 581.
42. Paul, D. R.; Yampol'skii, Y. P. Polymeric Gas Separation Membranes; CRC Press, **1993**.